Thermochimica Acta 493 (2009) 96–104

Contents lists available at ScienceDirect

Thermochimica Acta

journal homepage: www.elsevier.com/locate/tca

Characterizations of self-combustion reactions (SCR) for the production of nanomaterials used as advanced cathodes in Li-ion batteries

Ortal Haik[a], Surendra K. Martha[a], Hadar Sclar[a], Zvi Samuk-Fromovich[a], Ella Zinigrad[a], Boris Markovsky[a], Daniela Kovacheva[b], Nikolay Saliyski[b], Doron Aurbach[a,*]

[a] Department of Chemistry, Bar-Ilan University, Ramat-Gan 52900, Israel
[b] Institute of General and Inorganic Chemistry, Bulgarian Academy of Sciences, Sofia, Bulgaria

ARTICLE INFO

Article history:
Received 29 January 2009
Received in revised form 29 March 2009
Accepted 15 April 2009
Available online 23 April 2009

Keywords:
Self-combustion reactions
Li-ion batteries
Cathode materials
Thermal analysis
DSC
ARC

ABSTRACT

In this work, self-combustion reactions (SCR) for the preparation of important cathode materials for rechargeable Li-ion batteries were investigated by thermal analytical tools (DSC, ARC, TGA), electron microscopy, XRD, various spectroscopies (MS, Raman, FTIR) and elemental analysis by ICP. The systems studied include solutions containing metal nitrates at the right stoichiometry and sucrose as a fuel, for the preparation of $LiMn_{0.5}Ni_{0.5}O_2$ (layered), $LiMn_{1.5}Ni_{0.5}O_4$ (spinel), $LiMn_{0.33}Ni_{0.33}Co_{0.33}O_2$ (layered), and $LiMn_{0.4}Ni_{0.4}Co_{0.2}O_2$ (layered). Similar products, which do not depend on the atmosphere of the processes (air or inert) were obtained by spontaneous SCR and the gradual heating of the same solutions by DSC, ARC, and TGA. The reactions involve the partial caramelization of sucrose, complicated by red-ox reactions with the nitrates that form solid products, whose organic part is finally decomposed around 400 °C. The presence of cobalt ions has a stabilizing effect, which is expressed by the low dissolution rates of Li ions from the solid products thus formed, into aqueous solutions. The reaction mechanisms are discussed herein.

1. Introduction

Simple methods for synthesizing nano-sized mixed metal oxides by self-combustion reactions (SCR) of metal nitrates and some inorganic or organic reducing compounds (fuel) have been developed in recent years [1–9]. The main advantages are the good mixing between the atoms and the formation of nanosized clusters, whose further calcination produces nanoparticles of mixed metal oxides. The heat needed for the synthesis of these metal oxides is provided by the exothermic reaction between the fuel and the oxidizers, namely, the precursors that are the metal nitrates. Despite the wide use of this method for the preparation of a variety of pure and mixed oxides, most of the previous work was aimed at investigating the properties of the final products. At the same time, the mechanism of the self-combustion reaction itself is still not well understood. Moreover, the mechanism should strongly depend on the chemical and thermal properties of the metal nitrate precursors, and especially on the type of organic (or inorganic) fuel used. The transformation stages, the amount of the heat evolved during these reactions, the type and amount of gases produced, and their possible interactions, etc. are also unclear. For SCR using hydrazine as a fuel, it was claimed [1] that the reaction comprises steps of molecularly combining the nitrate precursors with the hydrazine to form metal nitrate–hydrazinate coordination compounds as the chemical precursors of the ceramic materials. Thereafter, these precursors exothermally decompose at temperatures lower than 200 °C, below the endothermic decomposition temperature of the nitrate species. Another example is the combustion synthesis for preparing CeO_2 powder. According to the authors [2] during the first stages of this reaction, ceric ammonium nitrate and urea decompose to gases such as NO_x, O_2, NH_3, HCNO, etc. Afterwards, exothermic gas phase reactions occur among these combustible species, resulting in acceleration of the entire combustion reaction process.

There are descriptions of SCR as multi-step reactions, beginning with a direct reaction between the nitrates and the fuel, followed by further reactions of the products [9]. It was also suggested that the mode of ignition of SCR, i.e., the gradual or sharp temperature steps, are not so important in determining the final products. There are reports on the use of DSC, DTA, TGA, and MS for such studies [2,3,9,10].

In the present work, we explored the details of SCR for preparing cathode materials for lithium ion batteries from metal nitrates and sucrose ($C_{12}H_{22}O_{11}$) as the reducing reagent [8]. These reactions were investigated by thermal, analytical, microscopic, diffraction and spectroscopic techniques. The SCR processes described in this work are indeed excellent tools for producing a wide variety of important cathode materials for advanced Li-ion batteries as nano-

* Corresponding author. Tel.: +972 3 5318317; fax: +972 3 7384053.
E-mail address: aurbach@mail.biu.ac.il (D. Aurbach).

0040-6031/$ – see front matter © 2009 Elsevier B.V. All rights reserved.
doi:10.1016/j.tca.2009.04.008

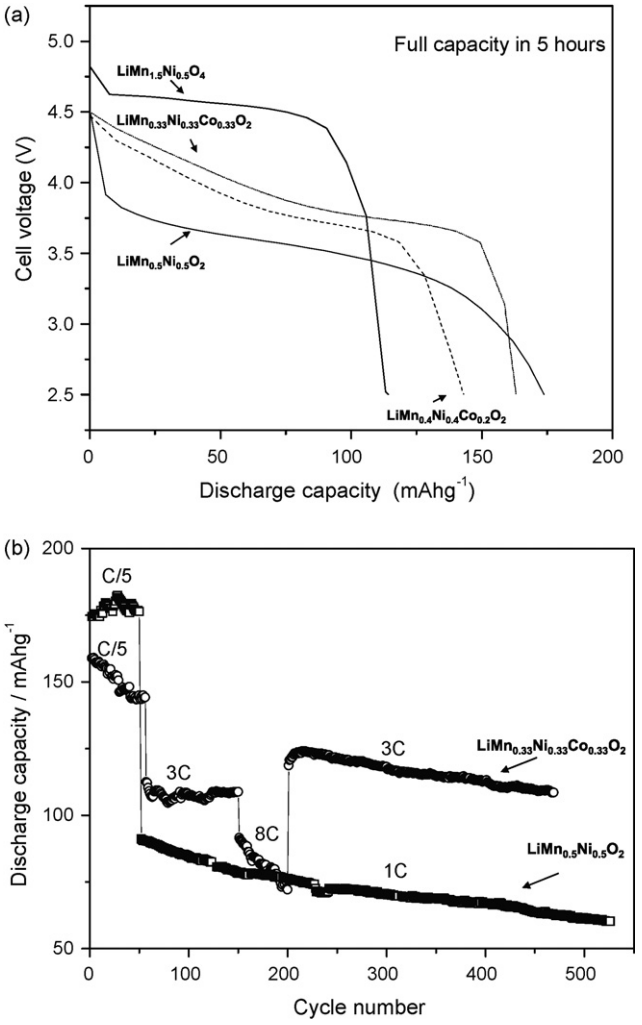

Fig. 1. Typical electrochemical behavior of electrodes comprising $LiMn_{0.5}Ni_{0.5}O_2$, $LiMn_{1.5}Ni_{0.5}O_4$, $LiMn_{0.4}Ni_{0.4}Co_{0.2}O_2$, and $LiMn_{1/3}Ni_{1/3}Co_{1/3}O_2$ nanometric powders as the active mass (indicated), vs. Li counter electrodes. Coin type cells with standard EC-DMC/1.5 M $LiPF_6$ solutions, $T = 30\,^{\circ}C$. (a) Steady state potential profiles (E vs. capacity curves) upon discharge at C/5 rate (lithiation); (b) galvanostatic cycling behavior at various discharge rates.

particles whose size (nano → micro) can be further fully controlled by the final calcination step. Moreover, the possibility to obtain such a variety of cathode materials by the same relatively simple synthesis, enables a reliable comparison among various cathode materials thus carrying out correctly the selection of optimal electrodes' materials. In our previous works [11,12] we demonstrated a superior rate capability of $LiMn_{1/3}Ni_{1/3}Co_{1/3}O_2$ cathodes and good cycling behavior of both $LiMn_{0.5}Ni_{0.5}O_2$ and $LiMn_{1/3}Ni_{1/3}Co_{1/3}O$ electrodes (see Fig. 1), which active mass was produced by SCR. Very good cycling efficiency and stability were obtained with $LiMn_{1.5}Ni_{0.5}O_4$ and $LiMn_{0.4}Ni_{0.4}Co_{0.2}O_2$ electrodes as well. Hence, the superior electrode materials thus obtained provide the incentive for the rigorous study of SCR. The work is aimed at providing a better and more complete picture of the self-combustion reactions of metal nitrates and sucrose and explaining their calorimetric response. We report herein on the synthesis of mixed oxides that are important cathode materials for advanced Li-ion batteries, namely materials from the Li–Ni–Mn–O family with a layered structure, $LiNi_{0.5}Mn_{0.5}O_2$, and spinel, $LiNi_{0.5}Mn_{1.5}O_4$. We also investigated syntheses by the SCR of two layered oxides from the Li–Ni–Mn–Co–O family comprising a different amounts of cobalt: $LiMn_{0.4}Ni_{0.4}Co_{0.2}O_2$ and $LiMn_{1/3}Ni_{1/3}Co_{1/3}O_2$.

2. Experimental

For the thermal analyses we used the following instrumentations: an accelerating rate calorimeter (ARC) from Arthur D. Little Inc., Model 2000; differential scanning calorimeters (DSC) from Mettler Toledo Inc., Models DSC 822 and DSC 25; a thermogravimetric analyzer (TG, DTA, SDT 2960, TA instrument). The reaction products were characterized by the following techniques: Fourier transform infrared (FTIR) spectroscopy (Magna 860 Spectrometer from Nicolet Inc.); elemental analysis by an inductively coupled plasma (ICP) spectrometer (Ultima 2, Jobin Yvon Horiba); X-ray diffraction using a D8 Advance System from Brucker Inc. (XRD patterns were obtained using Cu Kα radiation λ = 1.5418 Å at 40 mA and 40 kV); high-resolution scanning electron microscopy (HRSEM JEOL-SM-7000F electron microscope equipped with an energy dispersive X-ray microanalysis system from Oxford Inc.); Raman spectroscopy (a micro–Raman spectrometer HR800 from Jobin Yvon Horiba, using holographic grating, 1800 grooves/mm, with a He–Ne laser (excitation line 632.8 nm, 0.9 mW, and a 50x objective with a numerical aperture of 0.75. Each Raman spectrum presented in this work is an average of at least 3 scans of 1 min each; TGA–DTA–MS (thermogravimetry–mass spectrometry, TA TGA Q500 combined with Mass spectrometer (MS), model Thermostar, Pfeiffer).

DSC and TGA–DTA–MS experiments were performed under air and nitrogen atmosphere in order to check the possible influence of atmospheric components on the process. The gas flow in all of these measurements was 20 ml min^{-1}.

The reagent mixtures for the preparation of the nano-lithiated-oxide materials, $LiMn_{0.5}Ni_{0.5}O_2$, $LiMn_{1.5}Ni_{0.5}O_4$, $LiMn_{1/3}Ni_{1/3}Co_{1/3}O_2$ and $LiMn_{0.4}Ni_{0.4}Co_{0.2}O_2$, contained the stoichiometric amounts of the corresponding metal nitrates (oxidants) and sucrose (fuel) with an oxidant/fuel ratio = 1:1 in water. The pristine solutions, containing these metal nitrates at the right stoichiometry and sucrose, are denoted as A, B, C, and D, respectively. The concentrations of the reagents were adjusted to start the reactions with solutions containing 1 M $LiNO_3$. The reagents' purity was as follows: lithium nitrate (99%), nickel nitrate hexahydrate (97%), manganese nitrate tetrahydrate (97%), cobalt nitrate hexahydrate (98%), and sucrose (99.9%), all from Aldrich. The thermal reactions (with the above solutions) were carried out in five routes:

1. By self-combustion reaction in glass vessels, in which the starting (pristine) solutions (green in color) were heated by hot plate thermo-stated at 150 °C while being vigorously stirred. Spontaneous exothermal reactions are thus ignited bringing the reaction mixture to 400 °C and flame and pronounced gas evolution are involved.
2. By gradual heating the pristine solutions in DSC, ARC, TGA and TGA–MS instruments (four different routes, using appropriate containers).

In order to carry out these reactions, which produce a large amount of gases, the ARC measurements were conducted in opened containers (titanium). The opened containers were produced by cutting (to halves) standard titanium bombs for ARC (8.3 ml, Arthur D. Little Inc.). The samples were heated from 40 to 400 °C in 5 °C increments at the rate of 2 °C min^{-1} in the search for the onset of self-heating reactions at a sensitivity threshold of 0.02 °C min^{-1}. The controller was programmed to wait 15 min for the sample and the calorimeter temperatures to equilibrate, and then to search during 20 min for a temperature increase of 0.02 °C min^{-1}. Two series of DSC measurements were carried out using opened, reusable high-pressure crucibles; reactions in gold-plated stainless steel crucibles, 30 μl in volume, were measured by a DSC 822 instrument. Reactions in bigger, opened, reusable high-pressure crucibles were made of

a nimonic alloy (NiCr 20 TiAl), 270 μl in volume, were measured by the DSC 25 instrument. About 1 or 25 mg of solutions, respectively, were loaded into the crucibles and heated from 40 to 450 °C. The initial and final weights were measured using a microbalance (Mettler Toledo AB135-S/FACT). Heating/cooling rates of 0.5, 1, 10, and 20° C min^{-1} were employed. The most significant and comprehensive data were obtained at heating/cooling rates of 1 and 10 °C min^{-1} in measurements with the DSC 822 system, and of 1 °C min^{-1} in measurements by with a DSC 25 instrument. TGA and TGA–DTA–MS experiments were carried out in Pt plates or in alumina crucibles, 70 μl in volume, in a temperature range of 40–1000 °C. The amounts of solution loaded into the crucibles were about 1, 25 or 10 mg. TGA–DTA–MS tests were conducted with heating rates of 1 and 10 °C min^{-1}. Electrochemical measurements with the lithiated transition metal oxides thus produced were conducted as follows:

Composite electrodes were prepared by spreading slurries comprising the active mass, carbon powder and poly-vinylidene difluoride (PVdF) binder (ratio of 8:1:1 by weight, dissolved in N-methyl-2-pyrrolidone (NMP), onto aluminum foil current collector, following drying in a vacuum oven. The average load was around 2 mg active mass per cm^2. These electrodes were tested in two electrodes coin type cells (model 2032 from NRC Canada) with Li foil serving as the counter electrodes and standard electrolyte solutions: EC–DMC 1:1, 1 M $LiPF_6$ from Tomiyama Inc. (Japan). Computerized multi-channel battery analyzer from Maccor Inc. (USA) was used for galvanostatic measurements (voltage vs. time/capacity, measured at constant currents) at different rates and prolonged charge–discharge cycling.

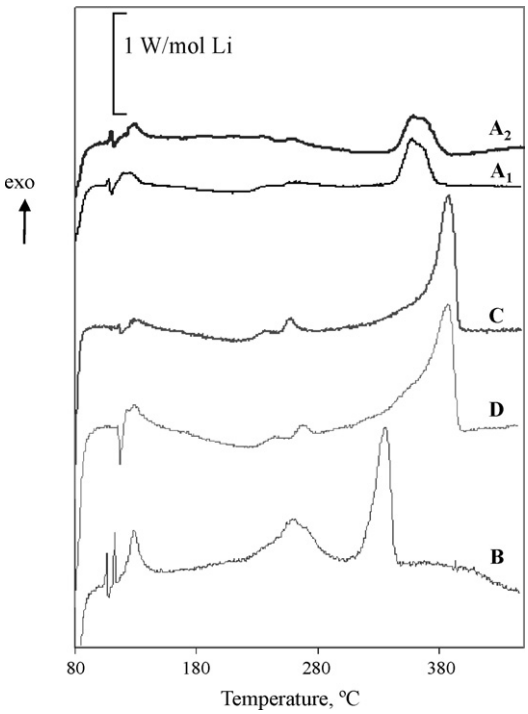

Fig. 2. DSC curves (measured with a DSC25 instrument) for solutions $A_{1,2}$–D, as indicated, from which $LiMn_{0.5}Ni_{0.5}O_2$, $LiMn_{1.5}Ni_{0.5}O_4$, $LiMn_{0.33}Ni_{0.33}Co_{0.33}O_2$, and $LiMn_{0.4}Ni_{0.4}Co_{0.2}O_4$ are prepared, respectively. A_1-conducted under N_2 atmosphere, and A_2-conducted under air atmosphere.

3. Results

3.1. On the similarity between spontaneous SCR and gradual heating of the metal nitrates/sucrose solutions

The main theme of this work was the use of combined thermal analytical methods for the study of self-combustion reactions between metal nitrates and sucrose, for the synthesis of the above important cathode materials. The typical self-combustion reaction is spontaneous and involves a flame ignited by heating the solutions in one step to 150 °C (hot plate), thus producing a solid product whose calcination (e.g., up to 700 °C) forms nanoparticles of the desired mixed metal oxides. When studying the corresponding solutions by DSC, ARC and TGA, the heating is gradual, what prevents the explosive type of reactions, but rather allows the study of their possible stages and mechanisms. The analysis of the products of the spontaneous SCR of all the solutions studied and the products of their heating by the three thermal analytical tools (DSC, ARC, TGA) showed very clearly that very similar products are obtained (for each solution), mostly the desired Li–Mn–Ni–O or Li–Mn–Ni–Co–O compounds. In some cases the products may also contain Li_2CO_3 and traces of $LiNiO_2$ or NiO. It is important to note that the atmosphere has no effect on these reactions and their products. This is clearly seen from the results in Fig. 2 A_1 and A_2, which correspond to reactions in air and nitrogen, respectively.

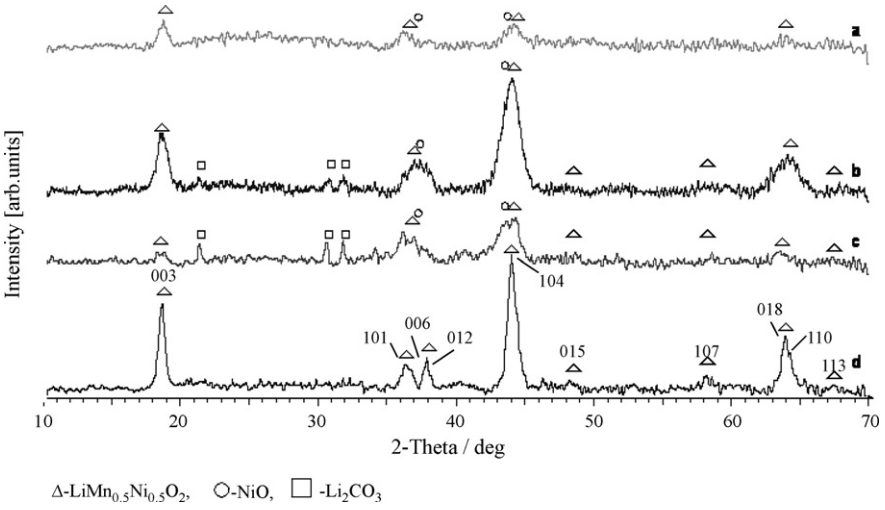

Fig. 3. XRD patterns of the various thermal products of solution A (for the preparation of $LiMn_{0.5}Ni_{0.5}O_2$). (a) 310 °C; (b) 450 °C; (c) the product of instantaneous SCR, solution heating on a hot plate at 150 °C, which ignites a spontaneous red-ox reaction that reaches 400 °C; (d) $LiMn_{0.5}Ni_{0.5}O_2$ produced by calcination at 700 °C during one hour (same product is formed by calcination of the SCR product or the product of gradual heating by DSC).

Table 1
The results of the XRD analyses of the products obtained by heating solution A (for the preparation of $LiMn_{0.5}Ni_{0.5}O_2$) to different temperatures (as indicated).

Heating rate, °C min^{-1}	End temperature, °C	*a* [Å] (main phase)	*c* [Å] (main phase)	*c*/*a*	Crystallite size [nm] (main phase)	Secondary phase
1	200	2.897 (3)	14.28 (5)	4.930		XRD peaks related to inter layer spacing of 3 Å
1	310	2.905 (4)	14.15 (4)	4.872	4.3 (3)	NiO
1	450	2.917 (1)	14.143 (9)	4.849	5.7 (1)	Li_2CO_3, NiO
20	450	2.924 (2)	14.09 (2)	4.819	6.3 (1)	NiO
30	450	2.929 (1)	14.076 (9)	4.806	6.5 (1)	NiO
1	700	2.893 (2)	14.336 (9)	4.955	15.2 (2)	

Hence, all data presented herein relate to reactions under nitrogen atmosphere.

Fig. 3 shows XRD patterns of the solid products obtained by the dynamic heating of solution A (from which $LiMn_{0.5}Ni_{0.5}O_2$ is prepared) by DSC up to 310, 400 and 450 °C (A–C, respectively), the product of SCR and SCR + calcinations to 700 °C of the same solution (D). The XRD patterns demonstrate the presence of an intermediate crystalline compound together with an organic phase, when the solution was heated up to 200 °C. The crystalline structure changes during further heating, as shown in the various XRD patterns (Fig. 3 and the data in Table 1). The analysis by XRD shows that a layered (inorganic) compound is formed when solution A is heated to 310 °C and then to 450 °C. The XRD patterns of the SCR product and the heating product by DSC to 450 °C are very similar and in fact similar also to the patterns of the calcinations product which is quite pure layered $LiMn_{0.5}Ni_{0.5}O_2$.

The Raman spectra of the gradual heating (by DSC) and the SCR products of solution A (Fig. 4) confirm the formation of a layered compound after heating solution A in DSC to 310 °C.

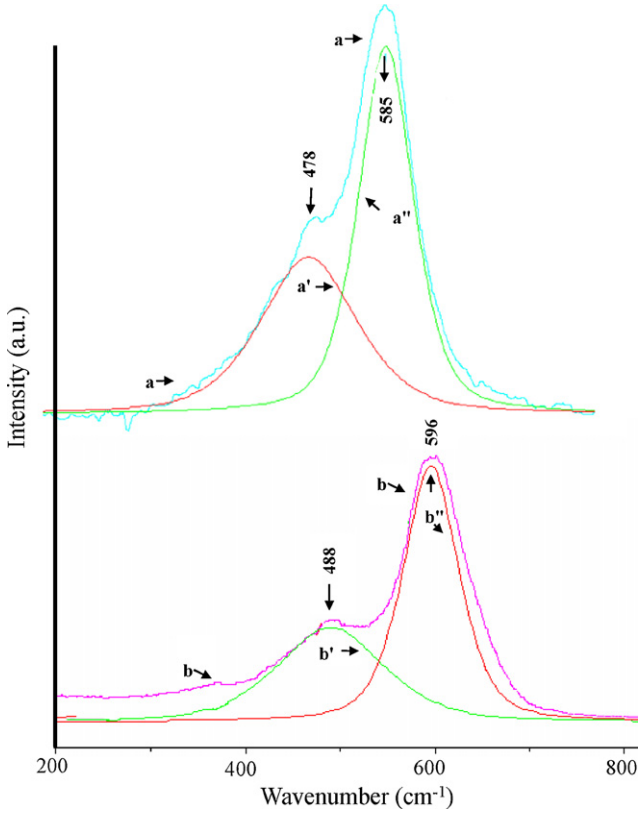

Fig. 4. Raman spectra of the heating products of solution A (for the preparation of $LiMn_{0.5}Ni_{0.5}O_2$). a, b – observed, a′, a″, b′, b″ – deconvoluted spectra, correspondingly. (a) Heating by DSC up to 310 °C. (b) The product of SCR obtained by heating solution A on a hot plate (150 °C) that ignites a spontaneous red-ox reaction.

Table 1 summarizes the results of the XRD analyses of the heating products of solution A. For the solid at 200 °C, it was difficult to refine the unit cell parameters since only the 0 0 3 peak is clearly seen in the pattern. The crystallite size for this sample was fixed to 50 nm in order to refine parameters. Additional XRD peaks corresponding to interplanar distances of 3 and 3.9 Å in the patterns of these samples, could be attributed to some unidentified organic components, not decomposed at this temperature. As the heating temperature is higher, the average crystallite size increases (Table 1). As indicated in this table, the XRD measurements show the formation of an additional NiO phase and in some cases Li_2CO_3 could also be detected. It should be noted that similar trends, including the formation of similar secondary phases, were observed from the XRD measurements of the solid products formed by heating solution C to different high temperatures. The XRD patterns presented in Fig. 5 related to solution D (for preparing $LiMn_{0.4}Ni_{0.4}Co_{0.2}O_2$) demonstrate that the products of the heating processes of the pristine metal nitrate–sucrose solutions by DSC (gradual heating, 1 °C min^{-1} rates) and by SCR are similar. The calcination products (e.g., produced upon heating tp 700 °C) are, nano-crystalline mixed oxide materials. Nevertheless, their XRD patterns resemble those of the SCR or the gradual heating products. What shows that the crystalline products are formed by SCR or by gradual heating beyond 300 °C. Hence, the similarity in the heating product of these solutions produced by different heating modes (DSC, ARC, SCR) is confirmed by XRD and Raman spectroscopic measurements and thereby, a further study of these reactions by the standard thermal analytical tools described below, seems to be justified.

3.2. Thermal measurements

We have found a consistent correlation between the ARC measurements of solution A for synthesizing $LiMn_{0.5}Ni_{0.5}O_2$ (figures are not shown) and the DSC curves of this solution measured at a heating rate of 1 °C min^{-1}. Using the dynamic heating mode allows a better separation between the second and the third exotherms. The four exotherms seen in the temperature range between 100 and 450 °C in Fig. 2 have onsets at about 110, 215, 250, and 345 °C, when the heating rate was 1 °C min^{-1}. The DSC curves obtained at the heating rates of 0.5, 1 and 10 °C min^{-1} are suitable for describing the thermal reactions, and demonstrate the same peaks, despite the shift to higher temperatures, $\Delta T = 30$ °C, as the heating rate is raised from 1 to 10 °C min^{-1}. At higher heating rates, e.g., 20 °C min^{-1}, the DSC response does not show resolved-enough pictures. Fig. 2 presents typical curves measured by a DSC 25 instrument of solutions A–D (for producing the four lithiated oxides studied herein) using higher sample weights, at a heating rate 1 °C min^{-1} (as indicated). These curves show a relatively similar behavior of all the four solutions studied. They exhibit broad endothermic peaks between 40 and 95 °C, related to the evaporation of excess water, narrow exothermic and endothermic peaks between 110 and 120 °C, and broad exothermic peaks around 130 °C, which end at about 140 °C. The next exothermic process is reflected by two merged consecutive

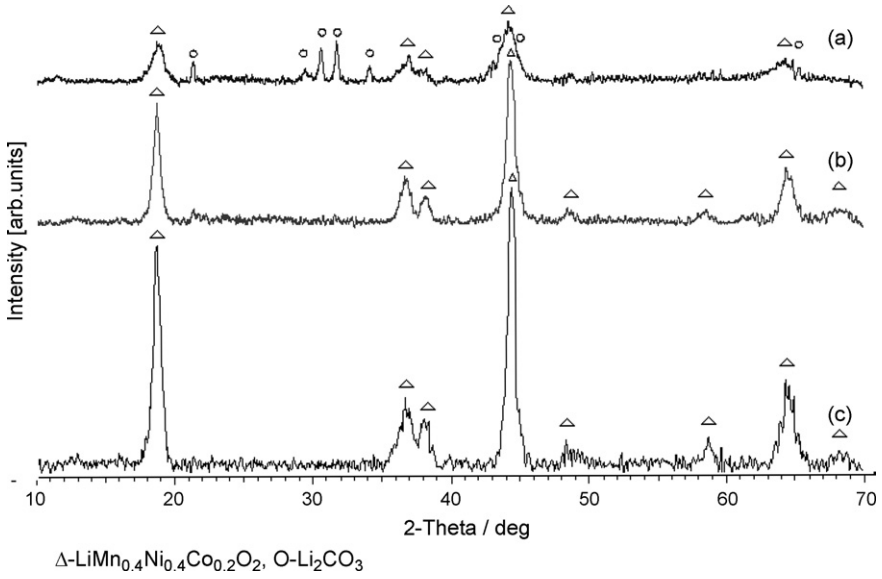

Fig. 5. XRD patterns of the heating products of solution D (for the preparation of $LiMn_{0.4}Ni_{0.4}Co_{0.2}O_2$). (a) Heating by DSC up to 450 °C, and (b) SCR product followed by calcination at 700 °C within 1 h. (c) Heating to 450 °C by DSC, followed by calcination at 700 °C within 1 h (nano-crystalline $LiMn_{0.4}Ni_{0.4}Co_{0.2}O_2$).

DSC peaks between 215 and 300 °C in the case of the layered materials (A, C, and D), and a single broad peak in the same temperature range for solution B, from which the $LiMn_{1.5}Ni_{0.5}O_4$ spinel material is formed. The biggest exotherm is seen beyond 300 °C and is related to the final step of the thermal reactions. The peak temperature of this process is the lowest for the $LiMn_{1.5}Ni_{0.5}O_4$ spinel structure (solution B), at about 335 °C, and is higher for solutions A, C and D from which the layered materials are prepared. It appears that the peak temperature obtainable upon self-combustion reaction of the solutions containing Mn, Ni and Li ions at ratio 1.5:0.5:1 (for preparing $LiMn_{1.5}Ni_{0.5}O_4$ spinel, solution B), is too low for the formation of the spinel structure upon the self-combustion reaction by itself. The $LiMn_{1.5}Ni_{0.5}O_4$ compound is obtained from solution B only rather SCR + further heating to threshold temperature of 360 °C. In contrast, self-combustion reactions of solutions A, C and D are sufficient for the formation of the layered structures studied herein. The peak shifts to the temperatures higher by 30 °C when cobalt is present in solution (solutions C and D). All the above-described peaks are irreversible, as proven by DSC measurements during cooling processes that were carried out at the end of the heating processes. DSC measurements of individual solutions of each component of the reactive mixtures (single metal nitrates and sucrose) are presented in Fig. 6. The concentration of components in these tests was equal to that in the pristine solutions (A–D). These data are in line with literature reports [13,14]. No observation of an endothermic decomposition of metal nitrates or sucrose in their pure aqueous solutions, as reflected by Fig. 6, indicates that the peaks in Fig. 2 are related only to thermal reactions between the metal nitrates and sucrose and not to individual components' decomposition. The overall specific heat measured for the three exothermic processes, detected between 115 and 400 °C for solutions A–D are 950, 2120, 3720 and 3100 J mol^{-1} of Li in solution, respectively (Table 2a).

There is a good agreement between the DSC, TGA and the MS measurements, carried out at a heating rate of 10 °C min^{-1} (Figs. 7–9). Preliminary experiments proved that this heating rate is appropriate for providing a significant MS response. In order to compare the DSC and the TGA–DTA–MS measurements, the former measurements were carried out in the DSC 822 system (small samples). TGA–DTA–MS and DSC curves recorded for solution A (Ni/Mn ion ratio = 1, for the production of $LiMn_{0.5}Ni_{0.5}O_2$) are shown in Figs. 7–9. The mass loss of 60% up to about 103 °C correlates well with the first endothermic peak of the evaporation of excess water (corresponding to a MS peak of $M/e = 18$), with the endset at about 103 °C. Fig. 7 shows TGA data as a % weight loss vs. T and the first derivative of this curve (indicated) for solution A. These TGA curves clearly show several consecutive weight losses when the solution is heated: below 100 °C and around 120, 160, 260, 400, 500, and 700 °C.

Fig. 8 compares the DSC curve of this solution and the derivative of the TGA curve (Fig. 7) in the temperature range of 80–400 °C. The comparison shows that the weight losses around 120, 160, 260 and 400 °C relate to a series of exothermal processes. The TGA–MS

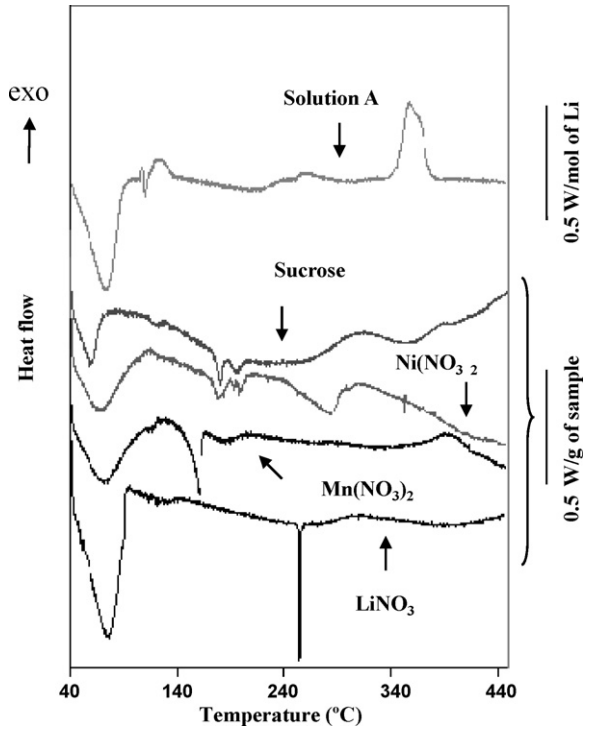

Fig. 6. DSC curves (measured with a DSC25 instrument) for various metal nitrate solutions, a sucrose solution and solution A for comparison, 1 °C min^{-1} (as indicated). Scale bars on Y-axis (shown at the right) are 0.5 W mol^{-1} of Li for a solution A and 0.5 W g^{-1} for a sucrose sample and metal nitrates solutions.

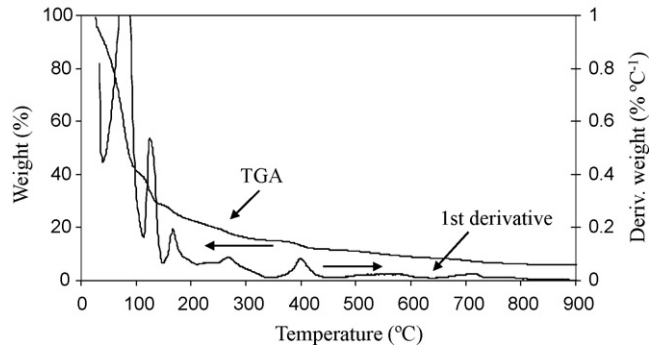

Fig. 7. TGA curves measured in air, 10 °C min^{-1}. The first derivative curves of the TGA data are also presented for clarification of the various thermal processes (as indicated).

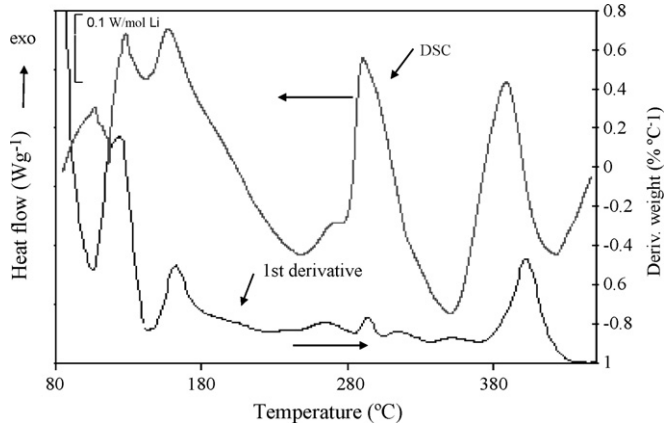

Fig. 8. Comparison between the DSC and TGA responses of solution A in the 80–430 °C temperature range. The TGA response is presented as the first derivative of the TGA curve, 10 °C min^{-1}.

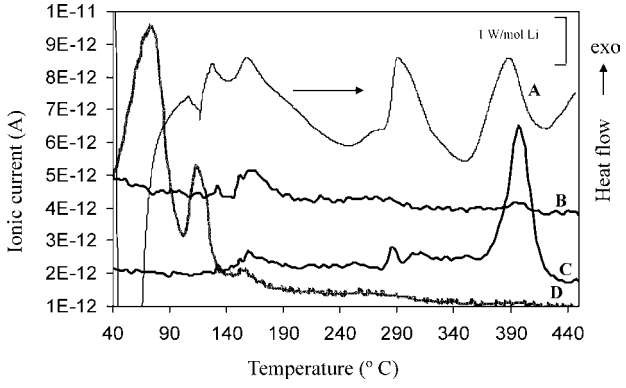

Fig. 9. DSC and TGA–MS response for solution A (for the preparation of $LiMn_{0.5}Ni_{0.5}O_2$) in the 40–330 °C temperature range, 10 °C min^{-1}. The TGA response is presented as the derivative of the TGA curve. (A) DSC curves; the MS response related to: (D) H_2O, (B) NO and (C) CO_2 (M/e = 18, 30 and 44, respectively) is presented.

response of the same solution, between 500 and 800 °C shows that the thermal processes around 550 and 700 °C seen in Fig. 7, involve evolution of CO_2. Fig. 9 compares the results of the DSC and TGA–MS measurements of solution A in the 40–440 °C temperature range with the emphasis on the MS responses of H_2O, NO and CO_2 (M/e = 18, 30, and 44, respectively). The results presented in Fig. 9 clearly demonstrate that the endothermic processes between 40 and 80 °C and around 120 °C (clearly reflected by DSC) relate to a loss of water (evaporation). These results also show that the exothermal processes between 120 and 180 °C involve the evolution of H_2O, NO and CO_2, while the exothermal processes around 300 and 400 °C involve mostly the evolution of CO_2. It can be said that the first thermal reaction after the evaporation of water, in which a significant mass loss occurs (30%) should be related to the second and third H_2O peaks (TGA–MS) that coincide with the TGA–MS peaks that reflect the evolution of CO_2 and NO. The simultaneous formation and evolution of H_2O, CO_2 and NO are related to the two exothermic processes around 130 and 160 °C, clearly seen by the DSC measurements. They should be related to the simultaneous caramelization process of sucrose [14–16] and to the red-ox reactions between the nitrates and the caramelization products. The two exotherms between 250 and 340 °C measured by DSC agree with the weight derivative peaks and with the further evolution of CO_2, NO and H_2O that cause the further weight loss of a few percent, measured in this temperature range. The last exothermic process with a peak temperature about 400 °C is also accompanied by CO_2 and NO evolutions and by a weight loss of a few percent. The calculated weight of the product formed after heating solution A to 450 °C is around 7.3% of the original weight (of the pristine solution). The weight loss % measured by the self-combustion reaction of the same solution, followed by calcination to 700 °C, was similar to that calculated from the TGA measurements.

Tables 2a and 2b present typical and representative results of the DSC and TGA measurements of solution A that were conducted under air and N_2 atmosphere. There is no evidence of any influence of the atmosphere on the thermal processes of these solutions. It should be emphasized that the picture in Figs. 7–9 presenting results related to solution A (comprising Li, Ni and Mn nitrates for the preparation of $LiMn_{0.5}Ni_{0.5}O_2$) is in general similar to that obtained with the other solutions, and hence, the data are representative.

3.3. Morphological and dissolution studies

In order to understand the path and mechanism of the self-combustion reactions, the solutions containing the metal nitrate and sucrose were heated up to 120, 160, 200, 310, and 450 °C, followed by product analysis. Upon heating, caramelization of the sucrose takes place in parallel to the evaporation of water, followed by reactions between the caramelization products and the nitrates (red-ox reactions) that form CO_2, H_2O and NO, as was evident from the TGA–MS measurements. These thermal reactions, form solids that become increasingly more inorganic in nature, and include an increasing portion of the metal ions as the temperature increases.

Table 2a
Parameters related to the reactions of solutions A–D obtained by the DSC measurements in temperature ranges (indicated) at a heating rate of 1 °C min^{-1}. The parameters were calculated as average of minimum five parallel DSC tests.

Solution	Peak temperatures of the four exothermic processes, °C					Total exothermic heat evolved in the second–fourth processes, J mol^{-1} of Li
	Temperature range, °C	First	Second	Third	Fourth	
A	218–385	130 ± 3	235 ± 2	258 ± 1	355 ± 4	950 ± 95
B	217–349	130 ± 3	235 ± 2		258 ± 1	2120 ± 90
C	220–404	130 ± 1	240 ± 3	265 ± 3	386 ± 4	3720 ± 300
D	224–402	130 ± 2	245 ± 2	265 ± 2	387 ± 2	3100 ± 300

End products: A—$LiMn_{0.5}Ni_{0.5}O_2$, B—$LiMn_{1.5}Ni_{0.5}O_4$, C—$LiMn_{0.33}Ni_{0.33}Co_{0.33}O_2$ and D—$LiMn_{0.4}Ni_{0.4}Co_{0.2}O_2$.

Table 2b
TGA parameters related to the reactions of solution A (1, 2, 3 relate to parallel experiments).

Test number	Weight loss, %					Residual mass at 1000 °C, %
	Temperature range, °C					
	Up to 120 Contributed to the loss of H_2O	120–140 Contributed to the loss of H_2O, CO_2, NO	140–300 Contributed to the loss of H_2O, CO_2, NO	380–430 Contributed to the loss of CO_2, NO	430–1000 Contributed to the loss of CO_2	
1	63	9	13	3	6	6
2	63	11	14	3	3	6
3	67	7	13	3	3	7

The effect of temperature on the content of metal ions in the solid and in the remaining liquid phase was studied by systematic ICP measurements. Upon heating, the pristine solution is transformed to a mixture of a brownish yellow mixture of syrup and foam, with the latter having a volume that is usually 5 times larger than that of the pristine solution.

The foam formed at temperatures below 160 °C is unstable and dissolves slowly in the liquid phase. Heating these solutions to temperatures higher than 160 °C forms foam, which does not dissolve in the residual liquid phase. The metastable black–gray porous solid thus formed shrinks gradually at room temperature. A brownish fragile solid is formed by heating up to 200 °C, which on further heating does not change the morphology of the solid thus formed, but rather changes its color (from brown to black).

The solids obtained after heating to 200, 250, 310, and 450 °C contain both organic products that dissolve in water and a solid phase that is only partially dissolved in water and in ethanol. FTIR spectra of the above various solid products were measured and discussed in the next section. However, displaying these spectra is not essential for the discussion. Solid samples formed by these heating processes were stored in distilled water or in dry ethanol at room temperature upon stirring during 15 min, and the resulting (brown) solutions were analyzed by ICP. As the heating temperature was higher, so the color of the aqueous solution (after storage of these solid samples) was pale. Fig. 10 presents the relative amount of metal ions in these solutions, as a function of the heating temperature (in which the solid product was formed), compared to the amount of these ions in the initial, pristine solutions whose heating formed the solid samples. The total amount of the ions in the pristine solutions was taken for these presentations as 100%. There is a pronounced dissolution of metal ions when the solid products produced at 200 and at 250 °C are put in contact with water (around 75 and 30%, respectively). The ease of dissolution of the metal ions from the solid product formed by heating of the pristine solution is a good measure of the formation of the inorganic metal–oxygen network, which is the precursor of the final $Li[MnNi]O_2$ or $Li[MnNiCo]O_2$ products. Dissolution of the metal ions from the solid phase formed at 310 °C is significantly lower compared to the above solid products (formed at lower temperatures). The solid phases formed at 310 and at 450 °C contain about 95% of the initial amount of metals. Li-ion dissolution from all the above-discussed solid products is much higher than that of Ni and Mn (Fig. 10). This can be explained not only by the much higher presence of Li in the organic phase (which dissolves in water), but also by the possibility of the chemical deintercalation of Li from the inorganic phase.

The content of Ni, Mn and Li in the compound formed at 700 °C is 100% (as compared to their content in the pristine solutions) The dissolution of the transition metal ions from the solids formed by calcination (>500 °C) to water or ethanol is zero, The level of the chemical deintercalation of Li in water reaches 41% for $LiMn_{05}Ni_{0.5}O_2$ even after calcination at 700 °C, and only 7% for $LiMn_{0.33}Ni_{0.33}Co_{0.33}O_2$ (Fig. 10). In fact, Fig. 10 reflects quite a complicated effect of the reaction temperatures on the stability of the solid products thus formed (as indicated by metal ions dissolution). For $LiMn_{0.5}Ni_{0.5}O_2$, there is no pronounced transition metal ion dissolution after temperatures beyond 320 °C are reached, while for $LiMn_{0.33}Ni_{0.33}Co_{0.33}O_2$ formation, only after a temperature above 360 °C is reached, the transition metal ions dissolution from the solid product thus formed becomes close to zero. However, as seen in Fig. 10b in the presence of cobalt in the solid product, Li-ions dissolution diminishes pronouncedly.

HRSEM micrographs of the solid product produced upon heating solution A up to 450 °C at a heating rate of 1 °C min^{-1}, show that it comprises nanometric flakes (Fig. 11). SEM micrographs of the solid product of solution A after calcination at 700 °C for 1 h show aggregated nanoparticles about 30–50 nm in size. Upon further heating of this material at 900 °C for 22 h, the particle size increases to about 300 nm in average. EDS measurements of all the solid products of solution A show a Ni/Mn ratio close to 1. The morphology of the final solid products of these solutions, formed either by gradual heating or by SCR followed by final calcination at temperatures around 700 °C and above, was the same.

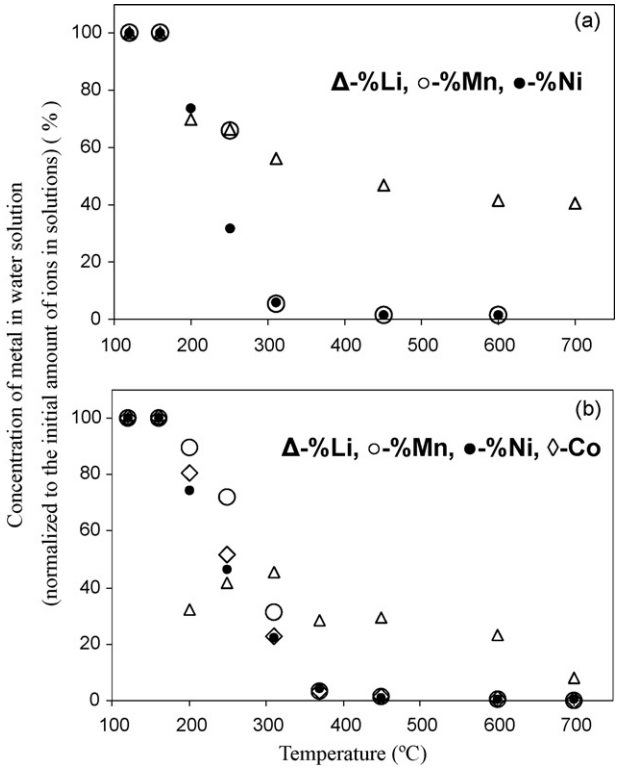

Fig. 10. The amount of the metal ions (Li, Ni, Mn, Co) according to ICP results, dissolved upon storage of the solid products formed by heating solutions A and C to different temperatures in distilled water. The amount of ions dissolved is normalized to the amount of ions in the initial solutions. (△) Li, (○) Mn, (●) Ni, (♦) Co. (a) Solution A (to form $LiMn_{0.5}Ni_{0.5}O_2$). (b) Solution C (to form $LiMn_{0.33}Ni_{0.33}Co_{0.33}O_2$).

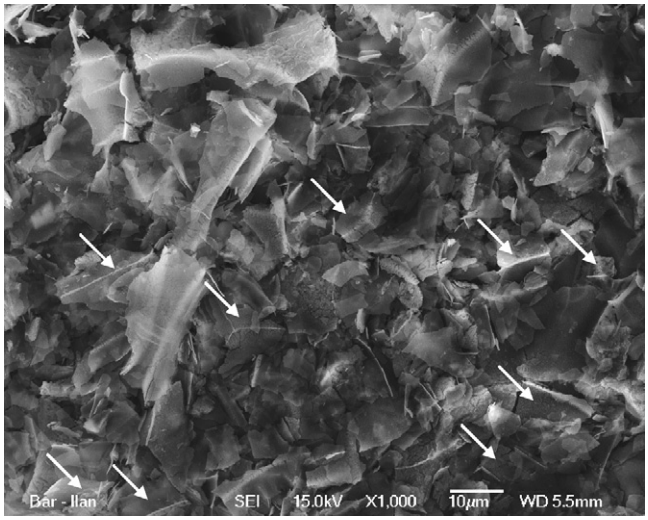

Fig. 11. HRSEM micrographs of the product of solution A (to produce $LiMn_{0.5}Ni_{0.5}O_2$) formed by heating to 450 °C. Arrows show grains of Li_2CO_3.

4. Discussion

The use of thermal analytical methods, including DSC, ARC and TGA in which the heating process is gradual, for the study of the SCR reactions between metal nitrates and sucrose (to form Li–Mn–Ni–O and Li–Mn–Ni–Co–O compounds), which are spontaneous and instantaneous, was found to be fully justified. Similar products are obtained by SCR and by heating in the framework of DSC, ARC and TGA measurements. The nature of the atmosphere has no effect on the products of these reactions. Major reactions occur at temperatures much lower than those needed for the decomposition of nitrates. An obvious reaction that takes place is the caramelization of the sucrose [14–16]. An obvious stage in the thermal reaction of sucrose is its decomposition to glucose and fructose:

$C_{12}H_{22}O_{11}$ (sucrose) + H_2O (water) → $C_6H_{12}O_6$ (glucose) + $C_6H_{12}O_6$ (fructose). A series of condensation stages then takes place to form species such as Caramelans ($C_{24}H_{36}O_{18}$), Caramelens ($C_{36}H_{50}O_{25}$), and Caramelins ($C_{125}H_{188}O_{80}$) via the liberation of H_2O and CO_2 [14–16]. In the reactions studied herein, these caramelization reactions are influenced or even catalyzed by the presence of metal nitrate in solutions. The FTIR spectra of the heating products of all these solutions up to 120 °C still resemble those of sucrose, fructose and glucose. However, the presence of IR bands between 1600 and 1800 cm^{-1} is highly significant, which belong to various carbonyl groups, and between 1900 and 2200 cm^{-1}, which belong to N–C double and triple bonds. These reflect complicated red-ox reactions between the nitrates and the sugar moieties. The FTIR spectra of the products of heating these solutions up to 200 °C show no υ_{CH} or υ_{C-O} peaks, but rather broad peaks around 1800–1600 and 1500–1900 cm^{-1}, which probably belong to condensation products that contain double bonds of C, O and N. These spectral results and conclusions are in line with the fact that there is no water loss above 140 °C (see Fig. 9). However, exothermal decomposition around 400 °C liberates CO_2 and NO (Fig. 9).

Hence, it can be assumed that the exothermal reactions indicated by the thermal studies described herein in the temperature range of 120–140 °C (Figs. 2, 6–9) relate to the combination of nitrates with sucrose (under air or nitrogen atmosphere), to form a metal nitrates–caramel coordination compounds which are the chemical precursors of the mixed metal oxide products. This scenario is confirmed by the simultaneous evolution of water, CO_2, and NO at temperatures that are lower than those of the thermal decomposition of nitrates or the full caramelization of sucrose [14,15]. The absence of a notable amount of nitrates and sucrose in the reaction mixtures at a temperature higher than 140 °C (Fig. 6) is a voidance for the completion of the reactions between nitrates and sucrose below this temperature. There are significant exothermal processes between 220 and 300 °C, accompanied by weight loss and gas evolution (NO, CO_2), related to the decomposition and transformation of the metals–oxygen–carbon–nitrogen complexes (unidentified) into inorganic composites, which structure approach that of the final crystal structure of the end products. Studies of solution A show that above 310 °C, the layered Li–Mn–Ni–O compound is the main product, together with a small amount of nickel oxide and an organic phase that contains no more than 5% of Ni and Mn and small amounts of Li and nitrogen. Between 340 and 390 °C, the most pronounced exothermal processes take place, accompanied by the evolution of CO_2 and NO, and by the formation of a small amount of Li_2CO_3. The formation of Li_2CO_3 may have two reasons—reaction of highly reactive Li_2O with some residual CO_2 within the sample, and second—reaction of Li_2O with the CO_2 from the air if the sample is exposed to air for some time before the XRD. In the second case, Li_2CO_3 crystals should be formed on the surface of the solid product. The final loss of carbonaceous species occurs between 450 and 650 °C. This is well reflected by the SEM studies, which show significant morphological changes due to the disappearance of the organic phase. The evolution of CO_2 upon heating the reaction products beyond 600 °C should relate to the decomposition of Li_2CO_3, which is formed at lower temperatures, to CO_2 and Li_2O. The onset temperature of the spontaneous endothermic decomposition of Li_2CO_3 is ≈650 °C [17,18]. The formation of $LiNiO_2$ due to calcination at high temperatures may result from the interaction between Li_2O and NiO, as the latter is absent when $LiNiO_2$ is detected.

The presence of Co ions in solutions (i.e., solutions C and D) does not change the onsets of the first three exothermal processes discussed above. However, the presence of Co ions increases the peak temperature of the fourth exothermal process around 350–400 °C. (Compare the DSC curves related to solutions A and C in Fig. 2). Highly interesting is the effect of the presence of cobalt ions in the solutions on the ease of the dissolution of the metallic ions from solid products formed at different temperatures, as reflected by the dissolution tests (solid product + distilled water, followed by element analysis of the water by ICP, Fig. 10). In the absence of Co ions, e.g., solution A, the transition metal ions (Ni, Mn) are strongly bound to the solid products formed at temperatures beyond 320 °C. However, the lithium ions are highly soluble, even from the product of calcination at 700 °C. In contrast, when Co ions are present (e.g., solution C, see Fig. 10), transition metal cations are no longer dissolved from the solid product formed upon heating beyond 350 °C and Li-ion dissolution (into aqueous solutions) from the solid products containing cobalt ions formed at high temperatures is remarkably less pronounced compared to the systems containing only Mn and Ni ions. Hence, it seems that the presence of Co ions has a stabilizing effect on the SCR products. This may correlate to the effect of cobalt ions on the electrochemical performance of the layered compounds. $LiMn_{0.33}Ni_{0.33}Co_{0.33}O_2$ is a much faster cathode material than $LiMn_{0.5}Ni_{0.5}O_2$, which is attributed to some ordering and lack of mixing between Ni and Li ions in the Li-ion layers, due to the presence of cobalt in the compounds [11]. The stabilizing effect of the presence of cobalt in the $Li[MnNiCo]O_2$ materials as reflected by the dissolution tests seems to correlate to the overall heat of formation of these materials. The overall specific heat of the formation of these layered materials between 115 and 400 °C increases with increase in the Co content in the compound. It equals to 950, 3100 and 3720 J mol^{-1} of Li for the syntheses of $LiMn_{0.5}Ni_{0.5}O_2$, $LiMn_{0.4}Ni_{0.4}Co_{0.2}O_2$ and $LiMn_{0.33}Ni_{0.33}Co_{0.33}O_2$ by SCR, respectively. This increase in the heat of formation of these compounds as the content of cobalt in the compound is

higher, means that the presence of Co in the compounds stabilizes them.

Another important finding that is clearly evident from this work is the pronounced difference between the SCR that forms the layered compounds and the similar reaction that forms the $LiMn_{1.5}Ni_{0.5}O_4$ spinel compound (see Fig. 2). This is expressed by pronounced exothermal reactions characterized by peak temperatures between 355 and 390 °C for the layered compounds, and the much lower peak temperature of the main exothermal process at 335 °C for the spinel samples.

5. Conclusion

We presented herein a systematic study of the thermal reactions of aqueous solutions containing lithium and transition metal (Mn, Ni, Co) nitrates and sucrose, which undergo self-combustion, an easy one-step versatile reaction to form a variety of lithiated transition metal oxides (e.g., $LiMn_{1.5}Ni_{0.5}O_4$ spinel, $LiMn_{0.5}Ni_{0.5}O_2$, and $LiMn_{0.33}Ni_{0.33}Co_{0.33}O_2$) as powders with nanometric-size particles. The average particle size of these products can be easily controlled by further calcination at temperatures above 700 °C (with the parameters T and t). These lithiated transition metal oxides can be used as advanced cathode materials with excellent electrochemical performance for rechargeable Li-ion batteries. In general, spontaneous combustion or gradual heating of these metal nitrate/sucrose solutions form the same products.

The solutions that include metal nitrates at the stoichiometry to form metal oxides with layered compounds (i.e., Li/Ni/Mn = $1:{}^1/_2:{}^1/_2$; Li/Ni/Mn/Co = $1:{}^1/_3:{}^1/_3:{}^1/_3$ or 1:0.4:0.4:0.2) demonstrate very similar thermal behavior, in terms of the type of processes and their onset temperatures. However, when the solutions contain cobalt ions, the specific heat evolution of their thermal reactions is higher (compared to that of the solution from which $LiMn_{0.5}Ni_{0.5}O_2$ is formed). The layered metal oxides are formed at temperatures > 300 °C. However, pure layered, lithiated transition metal oxides, suitable for use as Li batteries cathode materials are obtained only upon calcination at 700 °C (or above). The presence of cobalt stabilizes the layered compounds formed < 400 °C, as expressed by the fact that the spontaneous delithiation of the cobalt containing compounds in contact with water is relatively low. The stabilizing effect of cobalt is also well expressed by the higher heat of formation of the cobalt containing compounds. This may correlate to the fact that the Co containing layered oxides has improved performance in terms of high rate capability. Further work is needed for understanding such a correlation.

Acknowledgement

Partial support for this work was obtained by the ISF, the Israel Science Foundation.

References

[1] V.P.R. Verneker, Energy Citations Database (ECD), patent US 4751070, OSTI (1986).
[2] C.C. Hwang, T.H. Huang, J.S. Tsai, C.S. Lin, C.H. Peng, Mater. Sci. Eng. B 132 (2006) 229–238.
[3] S. Gopukumar, K.Y. Chung, K.B. Kim, Electrochim. Acta 49 (2004) 803–810.
[4] H.R. Sanu, G.R. Rao, Bull. Mater. Sci. 23 (2000) 349–354.
[5] N.A. Dhas, K.C. Patil, J. Mater. Chem. 3 (1993) 1289–1294.
[6] W. Yang, G. Zhang, J. Xie, L. Yang, Q. Liu, J. Power Sources 412 (1999) 81–82.
[7] K. Lee, H. Choi, J. Lee, J. Mater. Sci. 20 (2001) 1309–1311.
[8] D. Kovacheva, H. Gadjov, K. Petrov, S. Mandal, M.G. Lazarraga, L. Pascual, J.M. Amarilla, R.M. Rojas, P. Herrero, J.M. Rojo, J. Mater. Chem. 12 (2002) 1184–1188.
[9] S. Biamino, C. Badini, J. Eur. Ceram. Soc. 24 (2004) 3021–3034.
[10] G. Ting-Kuo Fey, T. Yang-Da Cho, Prem Kumar, J. Mater. Chem. Phys. 99 (2006) 451–458.
[11] S.K. Martha, H. Sclar, Z. Samuk-Fromovich, D. Kovacheva, N. Saliyski, Y. Gofer, P. Sharon, E. Golik, B. Markovsky, D. Aurbach, A comparative study of electrodes comprising nanometric and submicron particles of $LiNi_{0.50}Mn_{0.50}O_2$, $LiNi_{0.33}Mn_{0.33}Co_{0.33}O_2$, and $LiNi_{0.40}Mn_{0.40}Co_{0.20}O_2$ layered compounds, J. Power Sources 189 (2009) 248–255.
[12] Y. Talyosef, B. Markovsky, R. Lavi, G. Salitra, D. Aurbach, D. Kovacheva, M. Gorova, E. Zhecheva, R. Stoyanova, J. Electrochem. Soc. 154 (2007) A682–A691.
[13] http://www.fscimage.fishersci.com/msds/05290.htm, Material Safety Data Sheet, Cobalt (II) nitrate hexahydrate.
[14] N.L. Pennington, C.W. Baker, N.L. Pennington, Sugar: A User's Guide Sucrose, Aspen Publishers Inc., 2008, pp. 56–57.
[15] M. Quintas, C. Guimarães, J. Baylina, T.R.S. Brandão, C.L.M. Silva, Innovative Food Sci. Emerg. Technol. 8 (2007) 306–315.
[16] Caramelization. Wikipedia, The Free Encyclopedia http://www.en.wikipedia.org/wiki/Caramelization.
[17] A. Berbenni, G. Marini, R. Bruni, Riccardi, Thermochim. Acta 346 (2000) 115–132.
[18] N.D. Topor, L.I. Tolokonnicova, B.M. Kadenatsi, J. Thermal Anal. Calorimetry 22 (1981) 221–230.